Development 135, 3923-3933 (2008) doi:10.1242/dev.024620

Temporal requirement of the alternative-splicing factor *Sfrs1* for the survival of retinal neurons

Rahul N. Kanadia[1,2], Victoria E. Clark[1], Claudio Punzo[1], Jeffrey M. Trimarchi[1] and Constance L. Cepko[1,2,3,*]

Alternative splicing is the primary mechanism by which a limited number of protein-coding genes can generate proteome diversity. We have investigated the role of the alternative-splicing factor Sfrs1, an arginine/serine-rich (SR) protein family member, during mouse retinal development. Loss of *Sfrs1* function during embryonic retinal development had a profound effect, leading to a small retina at birth. In addition, the retina underwent further degeneration in the postnatal period. Loss of *Sfrs1* function resulted in the death of retinal neurons that were born during early to mid-embryonic development. Ganglion cells, cone photoreceptors, horizontal cells and amacrine cells were produced and initiated differentiation. However, these neurons subsequently underwent cell death through apoptosis. By contrast, *Sfrs1* was not required for the survival of the neurons generated later, including later-born amacrine cells, rod photoreceptors, bipolar cells and Müller glia. Our results highlight the requirement of Sfrs1-mediated alternative splicing for the survival of retinal neurons, with sensitivity defined by the window of time in which the neuron was generated.

KEY WORDS: Alternative splicing, Sfrs1, Survival of retinal neurons, Temporal

INTRODUCTION

As the genomes of different organisms are sequenced and annotated it is becoming apparent that the complexity of an organism does not depend on the total number of protein-coding genes. The current estimate for the number of protein-coding genes in the mouse (~23,049) (http://www.ensembl.org/Mus_musculus/index.html) is similar to that in *Arabidopsis thaliana* (Seki et al., 2002). Thus, it has been proposed that the complexity of higher metazoans must arise via the regulation of these genes at the transcriptional and post-transcriptional level. Alternative splicing (AS) is the mechanism by which exons of a single gene can be spliced in various combinations to encode a diverse set of proteins. Indeed, 74% of all human genes are known to be alternatively spliced and different tissues exhibit varying degrees of AS (Cheng et al., 2005; Johnson et al., 2003; Kampa et al., 2004). Moreover, when one considers that a single gene can produce multiple isoforms, the number of proteins encoded by the genome will most likely be much higher than the current estimates. In humans, the mRNAs that are expressed in the central nervous system (CNS) are subjected to the highest degree of AS when compared with other mature tissues (McCullough et al., 2005). However, the role of AS in CNS development is relatively unexplored. Given the complexity of AS, combined with that of CNS development, it is important that a system employed to investigate this question should be accessible, well characterized during development and relatively amenable to functional perturbation.

The vertebrate retina is part of the CNS, yet is a relatively simple tissue with six neuronal cell classes (rod photoreceptors, cone photoreceptors, horizontal cells, bipolar cells, amacrine cells and ganglion cells) and one glial type (Müller glia) organized in a stereotypic manner. The birth order of each cell type is conserved, such that ganglion cells, cone photoreceptors and horizontal cells are among the first-born cell types, followed by amacrine cells, rod photoreceptors, bipolar cells and Müller glia (Rapaport et al., 2004; Sidman, 1961; Young, 1985a). The production of each postmitotic cell type begins in the central retina and expands from the center to the periphery (Rapaport et al., 2004; Young, 1985a; Young, 1985b). Moreover, retinal development has been the focus of many studies, leading to a better understanding of mechanisms that govern cell fate determination and differentiation (Cepko, 1996; Livesey and Cepko, 2001). Thus, the current investigation focuses on understanding the role of an alternative-splicing factor (ASF) called splicing factor arginine/serine-rich 1 (*Sfrs1*) in retinal development.

Sfrs1 belongs to a highly conserved arginine/serine-rich (SR) protein family of RNA processing factors found throughout metazoans and in plants (Zahler, 1999; Zahler et al., 1992). The role of *Sfrs1* in splicing has been well documented, but only recently has its role in any developmental context been investigated (Xu et al., 2005). In *C. elegans*, ablation of the *Sfrs1* homolog resulted in late embryonic lethality, suggesting that its function is non-redundant in at least one critical stage of development (Kawano et al., 2000; Longman et al., 2001). In mice, the loss of *Sfrs1* also resulted in embryonic lethality (Xu et al., 2005). A conditional knockout (cKO) mouse in which the *Sfrs1* gene was flanked with loxP sites (*Sfrs1*$^{fl/fl}$) has enabled functional studies of *Sfrs1*. Xu et al. have shown that loss of *Sfrs1* does not cause aberrant proliferation and/or cell death of cardiac progenitor cells and that embryonic heart development proceeds normally (Xu et al., 2005). However, during postnatal remodeling of the heart, aberrant splicing of specific target genes such as cardiac troponin T (*cTnT*; *Tnnt2* – Mouse Genome Informatics), the Z-line protein cypher (*Ldb3*) and Ca^{2+}/calmodulin-dependent kinase II δ (*CaMKIIδ*; *Camk2d*), resulted in physiological defects in the heart (Xu et al., 2005).

In this report, we show that *Sfrs1* is expressed in the developing mouse retina and is itself regulated by AS. We have identified a new isoform that is expressed during late embryonic development and continues to be expressed during postnatal retinal development. This

[1]Department of Genetics, Harvard Medical School, Boston, MA 02115, USA. [2]Howard Hughes Medical Institute, Chevy Chase, MD 20815, USA. [3]Department of Ophthalmology, Harvard Medical School, Boston, MA 02115, USA.

*Author for correspondence (e-mail: cepko@genetics.med.harvard.edu)

Accepted 2 October 2008

novel isoform lacks the SR domain that is crucial for the nuclear localization of the Sfrs1 protein (Kataoka et al., 1999; Lai et al., 2000; Lai et al., 2001). Furthermore, the present investigation employs the *Sfrs1*$^{fl/fl}$ mice created by Xu et al. to determine the role of *Sfrs1* in the developing mouse retina. To specifically ablate *Sfrs1* function during retinal development, the *Sfrs1*$^{fl/fl}$ mice were crossed to mice that express Cre recombinase under the regulation of the ceh-10 homeodomain-containing homolog (*Chx10*; *Vsx2*), a gene that is expressed in retinal progenitor cells (Rowan and Cepko, 2004). The loss of *Sfrs1* function resulted in a small eye at birth. We found that loss of *Sfrs1* function did not have a significant effect on proliferation. However, neurons generated during early embryonic development underwent apoptosis, whereas those generated after birth did not. Consequently, neurons generated in the embryo, such as ganglion cells, cone photoreceptors, horizontal cells and amacrine cells, were significantly reduced in the *Sfrs1*-cKO retina. By contrast, rod photoreceptors, bipolar cells, late-born amacrine cells and Müller glia survived in the *Sfrs1*-cKO retina. The subset of susceptible neurons was defined primarily by the time of their birth, a possible reflection of the temporal heterogeneity in gene expression that has been defined for retinal progenitor cells (Trimarchi et al., 2008).

MATERIALS AND METHODS

Animal procedures

To generate *Sfrs1*-cKO retinae, *Sfrs1*$^{fl/fl}$ mice were crossed to *Chx10*::*Cre* mice. Mice were genotyped for *Sfrs1* by PCR (Xu et al., 2005). The presence of the *Cre* allele was also confirmed by PCR (Rivera-Feliciano and Tabin, 2006). When mice were subjected to surgical procedures, all IACUC protocols to minimize pain during and after surgery were observed.

RT-PCR

Retinae from different developmental time points were harvested and total RNA prepared in Trizol following the manufacturer's protocol (Invitrogen). For cDNA synthesis, 5 μg of total RNA from retinae harvested at various time points was used (Kanadia et al., 2006). PCR to detect *Sfrs1* isoforms was performed with a forward (5′-ATGTCGGGAGGTGGTGTGATCC-3′) and a reverse (5′-CCAATCATCTTATGTACGAGAGCGAGATC-3′) primer for 30 cycles (95°C for 35 seconds; 58°C for 25 seconds; 68°C for 2 minutes). PCR to detect *Tnnt2* isoforms was performed as described previously (Kanadia et al., 2003).

In situ hybridization on sections and dissociated cells

In situ hybridization (ISH) on 16 μm cryosections and dissociated cells was performed as described previously (Trimarchi et al., 2007). All the probes used in this report are as published previously (Trimarchi et al., 2008; Trimarchi et al., 2007). For *Sfrs1* we employed a 3′ UTR probe corresponding to bp 1620-2639 in the clone NM_173374 in the NCBI database.

Immunofluorescence

For immunofluorescence (IF), 16 μm cryosections were first hydrated in phosphate-buffered saline (PBS, pH 7.4), followed by the immunohistochemistry protocol of Kim et al. (Kim et al., 2008). The dilutions of the primary antibodies were: chicken anti-GFP (1:2000) (Abcam); mouse anti-Pax6 (1:300) (Covance); rabbit anti-Chx10 (1:300) (Cepko laboratory); mouse anti-rhodopsin (4D2; 1:300) (Molday and MacKenzie, 1983); mouse anti-glutamine synthetase (1:300) (Chemicon); rabbit anti-red/green opsin (1:300) (Chemicon); and mouse anti-Ki67 (1:250) (BD Pharmingen).

Immunoblot

The nuclear/cytoplasmic extraction protocol from Pierce was employed on retinae (n=10) from different stages. Upon fractionation, 30 μg of protein was resolved on a 4-20% Tris-glycine gradient gel (Invitrogen), followed by transfer of the proteins to a positively charged nylon membrane (Invitrogen), which was then subjected to immunoblot analysis as described previously (Kanadia et al., 2006). The primary antibodies used were mouse anti-Sfrs1 (1:1000) (Lifespan) and mouse anti-Cugbp1 (1:500) (Abcam).

Electron microscopy

P0 pups were harvested in 0.1 M sodium cacodylate buffer (pH 7.4), followed by fixation in 2% paraformaldehyde (PFA) and 2.5% glutaraldehyde in 0.1 M sodium cacodylate buffer. Retinae were then processed by the Harvard Medical School Electron Microscopy Core Facility.

P0 electroporation

P0 pups were electroporated with pCAG-Cre and pCAG-LoxP-Stop-LoxP-GFP plasmids or pCAG-GFP plasmid alone (Matsuda and Cepko, 2004).

Viral infections

Retroviral vectors were generated by cloning *Cre* after the IRES in the pQC-H2B-GFP-IRES-MCS vector (Punzo and Cepko, 2008). All viruses were prepared as described previously (Cepko, 1989). E10 viral infections by ultrasound-assisted delivery in timed-pregnant *Sfrs1*$^{fl/fl}$ and/or *Sfrs1*$^{wt/wt}$ females were performed as described previously (Punzo and Cepko, 2008). P0 viral infections were performed as described previously (Matsuda and Cepko, 2004).

BrdU pulse labeling

A pregnant female at E16 was weighed and then injected with 3 μg of BrdU/g body weight. At P7, retinae were harvested and processed for BrdU staining by antigen retrieval as described by the manufacturer (Vector Labs). Next, the slides were fixed in 4% PFA for 20 minutes followed by two 5-minute washes with PBS. Slides were treated with 2M HCl for 30 minutes at room temperature, followed by a brief wash with 0.1 M boric acid (pH 8.5) and IF was performed as described previously (Kim et al., 2008).

RESULTS

Sfrs1 is expressed during retinal development and is itself regulated by alternative splicing

To understand the role of *Sfrs1* during mouse retinal development, we first characterized its expression pattern. RNA ISH was employed on sections from embryonic day (E) 10.5 to postnatal day (P) 30 (Fig. 1A). At E10.5 and E11.5, expression of *Sfrs1* was detected in progenitor cells. However, in the peripheral retina, *Sfrs1* expression did not extend to the edge, a portion of the retina that is known to give rise to the ciliary body (Davis-Silberman and Ashery-Padan, 2008). In addition, the ISH signal for *Sfrs1* was enriched in cells at the apical end of the retina (Fig. 1A, E10.5 arrowhead), where the retinal progenitor cells undergo the M phase of their cell cycle (Sidman, 1961; Young, 1985b). Similar asymmetric enrichment of the ISH signal for *Sfrs1* was observed in the olfactory epithelium (see Fig. S1 in the supplementary material). ISH for cell division cycle 20 (*Cdc20*), a marker of the G2–M phase of the cell cycle, and IF for phosphorylated histone H3 (PH3), a marker of M phase, were employed (see Fig. S1 in the supplementary material) to determine whether the region of *Sfrs1* expression in the olfactory epithelium was also the region of M phase (Kawauchi et al., 2005; Trimarchi et al., 2008; Weinstein, 1997). As predicted, both the ISH for *Cdc20* and IF for PH3 confirmed that the mRNA for *Sfrs1* was enriched in areas expressing these genes, thereby suggesting the involvement of *Sfrs1* in cells in the G2–M phase of the cell cycle. At E12.5, *Sfrs1* expression was expanded to the entire neuroblastic layer (NBL) (Fig. 1A) and was also observed in the lens epithelium. In addition, at E13.5, expression of *Sfrs1* was transiently enriched in cells lining the vitreal side of the peripheral retina (Fig. 1A, E13.5, arrowhead), but this expression pattern was no longer observed by E14.5, at which time the expression of *Sfrs1* in the ONBL persisted. At P0, the expression of *Sfrs1* was again in the ONBL (Fig. 1A). During postnatal development, the expression of *Sfrs1* was restricted to the newly forming inner nuclear layer (INL) in the central retina, while in the periphery the expression of *Sfrs1*

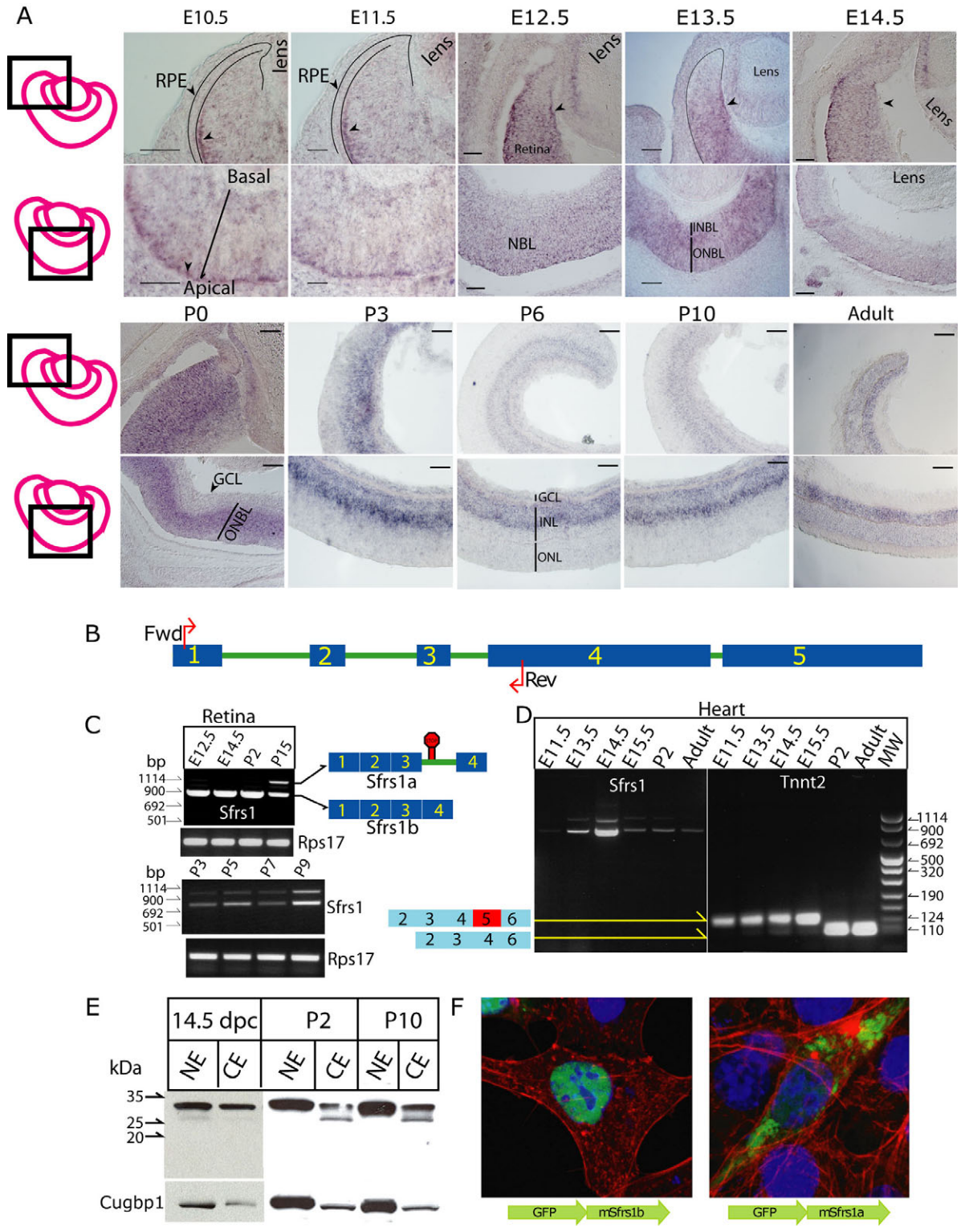

Fig. 1. *Sfrs1* expression during mouse retinal development. (**A**) In situ hybridization detecting *Sfrs1* RNA during retinal development. The schematic to the left indicates the location (box) of each row of images in the developing retina. Scale bars: 50 μm. (**B**) Schematic representation of the *Sfrs1* gene, showing exons (blue boxes, 1-5), introns (green lines) and the primers (red arrows) used for RT-PCR analysis. (**C**) Two RT-PCR products from the *Sfrs1* coding sequence. The bottom panel shows *Rps17*, which was used as a control. The top band for *Sfrs1* retains intron 3 (Sfrs1a), whereas the lower band is the canonical isoform with all four exons (Sfrs1b). (**D**) RT-PCR products of *Sfrs1* coding sequence from heart cDNA from different developmental stages are shown along with PCR products for *Tnnt2* as assessed by amplifying exon 2 to exon 6. (**E**) Immunoblot analysis (nuclear and cytoplasmic retinal extracts) to detect production of the new isoform of *Sfrs1* at E14.5, P2 and P10. Fractionation and equal protein loading were assayed by probing for Cugbp1. (**F**) Localization of the two isoforms of *Sfrs1* as achieved by fusing Sfrs1a and Sfrs1b with GFP followed by transfection of NIH3T3 cells. The cells are counterstained with phalloidin (red) and DAPI (blue).RPE, retinal pigmented epithelium; GCL, ganglion cell layer; NBL, neuroblastic layer; INBL, inner neuroblastic layer; ONBL, outer neuroblastic layer.

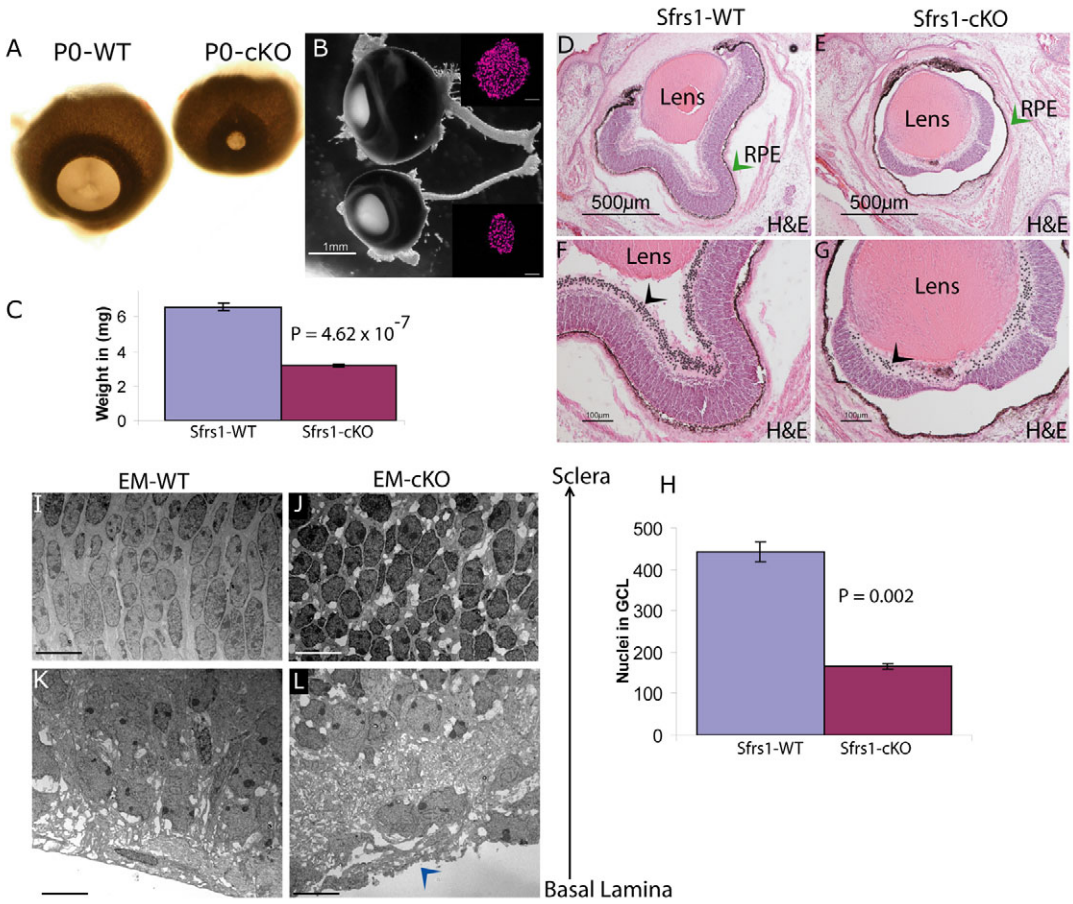

Fig. 2. *Sfrs1*-cKO mice have small eyes at P0. (**A**) Frontal view of wild-type (WT) and *Sfrs1*-cKO eyes. (**B**) Lateral view of the eyes and optic nerve. Insets show cross-sections of the optic nerves stained with DAPI (magenta). (**C**) Total weight comparison of wild-type (*n*=4) and mutant (*n*=4) eyes. (**D**,**E**) Hematoxylin and Eosin (H&E) stain of P0 wild-type and mutant retinae. Arrowhead indicates the retinal pigmented epithelium (RPE). (**F**,**G**) Higher magnification of D and E, with each ganglion cell nucleus marked with a dot (arrowhead) Scale bars: 100 μm. (**H**) Quantification of the ganglion cell layer cellularity in wild-type (*n*=3) and mutant (*n*=3) retinae. (**I-L**) Ultrastructural analysis of wild-type and mutant retina, with the basal lamina indicated in the mutant retina (J, arrowhead). Scale bars: 10 μm.

was observed in progenitor cells. At P6, *Sfrs1* expression became restricted to the lower half of the INL, where mostly amacrine and displaced ganglion cells are found, and to the ganglion cell layer (GCL), where ganglion and displaced amacrine cells are found (Fig. 1A). This pattern was also observed at P10 and P30 (Fig. 1A).

The expression of *Sfrs1* was also investigated by RT-PCR analysis. Recent reports have indicated that the protein level of most of the SR-protein family members is regulated by AS (Lareau et al., 2007; Ni et al., 2007). Thus, we investigated whether AS might modulate the protein levels of Sfrs1 during retinal development. To determine the AS status of *Sfrs1*, which has 5 exons (Fig. 1B), a forward primer in exon 1 (start codon) and reverse primer in exon 4 (stop codon) (Fig. 1B, red arrows) were utilized. Indeed, *Sfrs1* was found to be regulated via AS in a temporal manner, such that only one isoform (Sfrs1b) was observed in the embryo, whereas an additional isoform at a higher molecular weight (Sfrs1a) was also expressed postnatally (Fig. 1C). The temporal regulation of *Sfrs1* via AS led us to investigate whether a similar form of regulation was also employed during the development of other tissues. Because the role of *Sfrs1* in heart development has been investigated (Xu et al., 2005), this tissue was examined. RT-PCR analysis with the same primers showed that during embryonic heart development, both isoforms of *Sfrs1* were present. By contrast, the predominant isoform at P2 was the Sfrs1b isoform, which was also the only one expressed in the adult (Fig. 1D).

Sequence analysis revealed that Sfrs1b was the canonical isoform, whereas Sfrs1a retained intron 3. Consequently, in the Sfrs1a isoform there was a frame shift in the coding sequence resulting in the truncation of the RS domain. This change is of functional significance because Sfrs1 shuttles between the cytoplasm and the nucleus and the phosphorylation of the RS domain is required for its nuclear localization (Caceres et al., 1998; Ma et al., 2008). Thus, during retinal development, the AS of *Sfrs1* produces an isoform that would most likely fail to translocate into the nucleus. In agreement with the RT-PCR analysis, immunoblot analysis showed two immunoreactive bands in the cytoplasmic fraction from the postnatal, but not the embryonic, retina (Fig. 1E). In addition, the lower molecular weight isoform (Sfrs1a) of *Sfrs1* was significantly more abundant in the cytoplasmic than in the nuclear fraction (Fig. 1E). Since the Sfrs1a isoform was predicted to be cytoplasmic, the low-level detection of Sfrs1a in the nuclear fraction might be due to cross-contamination between the two fractions. The inability of the Sfrs1a isoform to shuttle into the nucleus was further investigated by fusing the coding sequence of Sfrs1a and Sfrs1b to GFP, followed

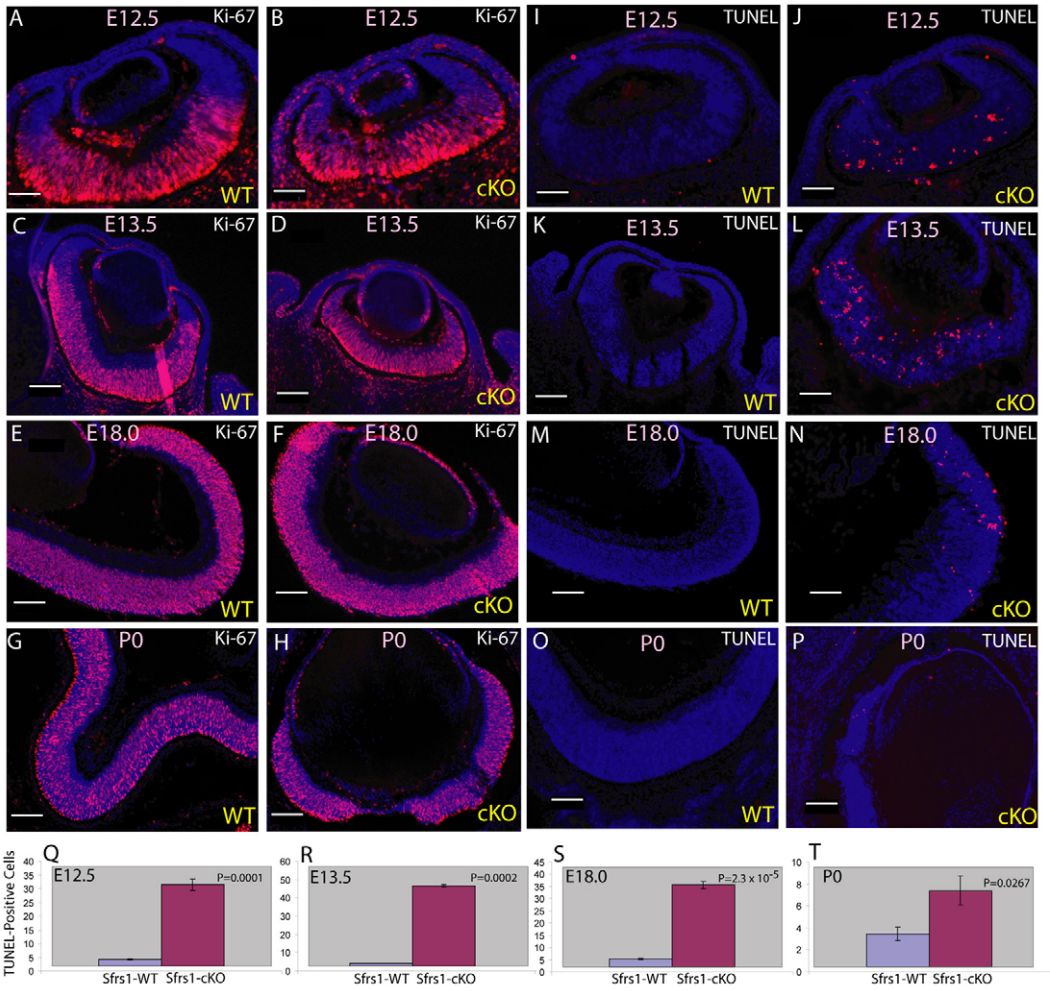

Fig. 3. Proliferation and cell death in *Sfrs1*-cKO mice. (**A-H**) Proliferation as determined by Ki67 immunofluorescence in wild-type (WT) and *Sfrs1*-cKO retinae at E12.5, E13.5, E18.0 and P0. (**I-P**) Cell death as determined by TUNEL analysis in WT and *Sfrs1*-cKO retina at E12.5, E13.5, E18.0 and P0. (**Q-T**) Quantification of the number of TUNEL$^+$ cells per section from different animals in the mutant retina as compared with the wild-type at E12.5 (n=4 for WT and *Sfrs1*-cKO), E13.5 (n=3), E18 (n=3) and P0 (n=5). Scale bars: 50 μm in A,B,I,J; 100 μm in C-H,K-P.

by transfection of each plasmid into NIH3T3 cells. As predicted, the canonical isoform, Sfrs1b, was predominantly located in the nucleus, whereas Sfrs1a was not observed in the nucleus (Fig. 1F). In summary, *Sfrs1* is expressed throughout retinal development and is regulated by AS in a temporal manner.

Sfrs1-cKO mice have small eyes at birth

The role of *Sfrs1* during retinal development was investigated by genetic ablation of *Sfrs1* function in retinal progenitor cells by crossing the *Sfrs1*$^{fl/fl}$ mouse to a *Chx10*::*Cre* transgenic mouse (Rowan and Cepko, 2004). Consequently, the majority of the developing retina lacked *Sfrs1* function. The *Sfrs1*-cKO retinae underwent aberrant embryonic development, which was inferred from the observation that *Sfrs1*-cKO mice were born with small eyes (Fig. 2A). *Sfrs1*-cKO eyes also had a thin optic nerve and the total eye weight was half that of the wild type (Fig. 2B,C). Hematoxylin and Eosin (H&E) staining of the retinal sections revealed a significant decrease in the size of the retina, but not in the retinal pigmented epithelium (RPE) or the lens (Fig. 2D,E). The retina was detached from the RPE (Fig. 2E, arrowhead) while abutting the lens and exhibited a marked decrease in the cellularity of the GCL, along with a perturbed inner limiting membrane (ILM) (Fig. 2G, arrowhead). Quantification of the number of nuclei in the GCL (Fig. 2F,G, arrowhead) confirmed the decrease in GCL cellularity (Fig. 2H), which in turn was reflected in the thin optic nerve (Fig. 2B, insets). Ultrastructural analysis showed that cells in the mutant retina were highly disorganized, with vacuolar inclusions, unlike the wild-type retina, which had elongated nuclei with a defined polarity (Fig. 2I-L). The absence of the ILM in the H&E-stained sections was confirmed by ultrastructural analysis (Fig. 2L, arrowhead). The mutant retina exhibited a dysmorphic fibrous layer instead of the well-organized ILM seen in the wild-type control retina (Fig. 2K). In summary, loss of *Sfrs1* function had a profound effect on the embryonic development of the retina and, possibly, also on that of the ciliary body, which together might have contributed to the microphthalmia observed at birth.

Sfrs1 loss-of-function causes cell death during embryonic retinal development

To determine the cause of the small retina in the *Sfrs1*-cKO mice at P0, we investigated whether the mutant retina had a proliferation defect during embryonic development. Ki67 antibody, a well-characterized proliferation marker (Gerdes et al., 1991), was employed on retinal sections from E12.5, E13.5, E18.0 and P0. No proliferation defect was observed in the *Sfrs1*-cKO retina (Fig. 3A-H). This was confirmed by quantification of the PH3 staining in the *Sfrs1*-cKO retina at E12.5 (see Fig. S2 in the supplementary material). Therefore, cell death was investigated as a cause of the small eye phenotype in *Sfrs1*-cKO mice. Terminal dUTP nick end labeling (TUNEL) assay revealed a significant increase in the number of TUNEL$^+$ cells at E12.5, E13.5 and E18.0 in the mutant retina (Fig. 3I-N). TUNEL$^+$ cells observed in *Sfrs1*-cKO retina at E12.5 and E13.5 were predominantly in the central retina (Fig. 3J,L), whereas the

majority of the TUNEL$^+$ cells at E18.0 were in the periphery (Fig. 3N). At P0, few TUNEL$^+$ cells were observed in the periphery (Fig. 3P). Furthermore, quantification of the TUNEL$^+$ cells in the mutant retina at each stage revealed that the cell death peaked at ~E13.5, followed by a decrease in the number of TUNEL$^+$ cells at E18, with few TUNEL$^+$ cells at P0 (Fig. 3Q-T). In summary, loss of *Sfrs1* function during embryonic development caused cell death and did not cause an observable reduction in proliferation; however, a subtle reduction in proliferation could not be ruled out.

Sfrs1 loss-of-function does not result in the death of retinal progenitor cells

There were three different scenarios that could explain the small eye phenotype. The dying cells might be progenitor cells, they might be postmitotic cells, or they might comprise both types of cells. Since proliferation was not reduced, it was unlikely that progenitor cells died. Nonetheless, this was investigated further because *Sfrs1* is expressed in progenitor cells during embryonic development. For this, *Sfrs1* function was ablated in retinal progenitor cells utilizing a retrovirus expressing Cre along with nuclear GFP (histone H2B-GFP fusion). Because retroviruses can only infect mitotic cells, the retinal progenitor cells would lose *Sfrs1*. Moreover, the viral genome inserts into the cell genome and thereby marks all its progeny. This retrovirus was delivered to E10.5 *Sfrs1*$^{fl/fl}$ embryos with the aid of an ultrasound-guided injection device, followed by detection of GFP immunofluorescence at P14 (Fig. 4). A virus encoding membrane-GFP (mGFP), without Cre, was also injected as a control for the infection. An additional control was to repeat the same experiment in *Sfrs1*$^{wt/wt}$ mice. Analysis at P14 showed several clones with nuclear GFP in the retinae of infected *Sfrs1*$^{fl/fl}$ mice (Fig. 4C), indicating the survival of the initially infected progenitor cells. However, there was a difference in the cell-type composition of the clones in the *Sfrs1*$^{fl/fl}$ and *Sfrs1*$^{wt/wt}$ mice. Based on their position, the majority of GFP$^+$ cells in the *Sfrs1*$^{fl/fl}$ mice were either rod photoreceptors, bipolar cells or Müller glia (Fig. 4C). By contrast, the cell types observed in the *Sfrs1*$^{wt/wt}$ mice, as determined by the position of the nuclei, included rod photoreceptors, horizontal cells, bipolar cells, Müller glia, amacrine cells and ganglion cells (Fig. 4B). The Cre-negative mGFP$^+$ clones were similar in composition to those of the wild type (data not shown). In conclusion, the loss of *Sfrs1* did not cause retinal progenitor cell death, at least not in all infected progenitor cells.

This conclusion was further bolstered by the genetic ablation strategy that employed the *Chx10*::*Cre* line along with a reporter line, *RC*::*PFWE*, in the *Sfrs1*$^{fl/fl}$ background. The *RC*::*PFWE* strain reports Cre activity by expressing nuclear β-galactosidase (*nlacZ*) (Farago et al., 2006). Thus, every progenitor cell that expresses Cre should be positive for *nlacZ* and negative for *Sfrs1* function. The results showed that at least some retinal progenitor cells did not die, as there were *nlacZ*$^+$ neurons in the P7 mutant retina (Fig. 4E). These neurons, as judged from their position, were mostly photoreceptors, bipolars and Müller glia (Fig. 4E). By contrast, the wild-type littermate retina showed many cells expressing *nlacZ* in the ONL (outer nuclear layer) (rod photoreceptors, cone receptors), INL (bipolar cells, horizontal cells, amacrine cells and Müller Glia) and in the GCL (ganglion and amacrine cells) (Fig. 4D). In both the wild-type and the mutant retinae there were cells that were negative for *nlacZ*, which was likely to result from the mosaic expression of *Chx10*::*Cre* (Rowan and Cepko, 2004). In summary, loss of *Sfrs1* function did not lead to the death of all progenitor cells, although some progenitor cell death could not be ruled out.

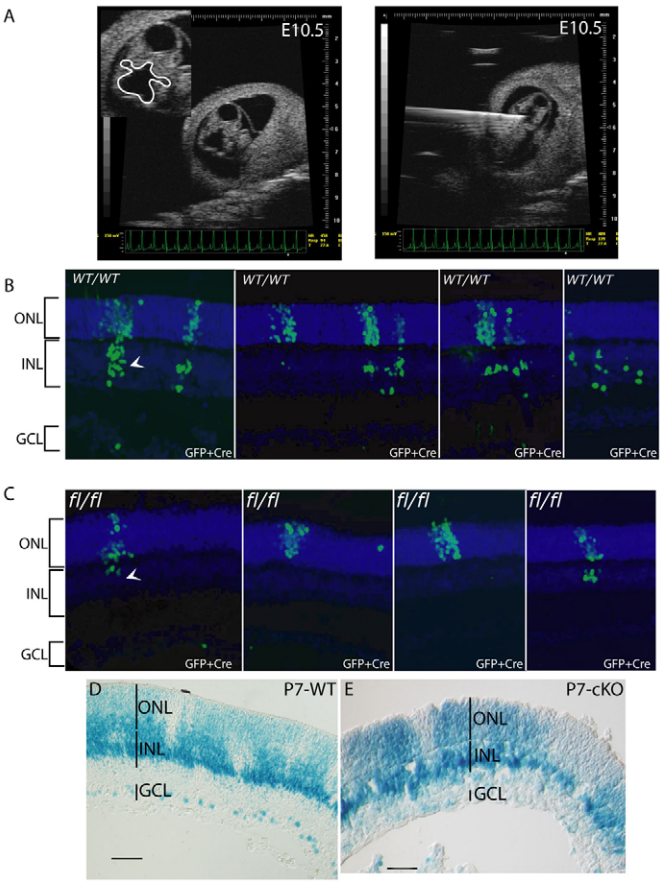

Fig. 4. Retinal progenitor cells survive the loss of *Sfrs1*. (**A**) Snapshot of a live ultrasound image of an E10.5 mouse embryo imaged through the uterine wall. Inset shows the newly formed optic vesicles and the diencephalon is traced in white. The right-hand panel shows a glass needle that was introduced into the ventricle where the virus was delivered. (**B**) P14 retinal sections from *Sfrs1*$^{wt/wt}$ embryos that were injected at E10.5 with a virus expressing Cre and nuclear-GFP. Stained for GFP. The arrowhead shows the position of the amacrine cells. (**C**) P14 retinal sections from *Sfrs1*$^{fl/fl}$ embryos injected at E10.5 with the same virus. The arrowhead highlights the absence of the amacrine cells. (**D**,**E**) P7 retinal sections from *Sfrs1*$^{wt/wt}$ and *Sfrs1*$^{fl/fl}$ mice that were crossed to the *RC::PFWE* line, which reports the *Chx10*::*Cre*-mediated excision event by activating *nlacZ* expression. GCL, ganglion cell layer; INL, inner nuclear layer; ONL, outer neuroblastic later. Scale bars: 50 μm.

Postmitotic cells are generated in the *Sfrs1*-cKO retina during early embryonic development

To examine whether the postmitotic cells were dying in the *Sfrs1*-cKO retinae, we first determined whether postmitotic cells were produced. For this, RNA ISH with probes that label differentiated neurons was employed on E13.5 retinal sections. First, loss of the *Sfrs1* transcript in the *Sfrs1*-cKO retina was confirmed (Fig. 5B). Although the majority of the retina lacked *Sfrs1*, a few cells (Fig. 5B, arrowhead) were positive for *Sfrs1*, most likely reflecting the *Chx10*::*Cre* mosaicism (Rowan and Cepko, 2004). ISH analysis was performed on serial sections with probes that mark postmitotic cells, including neurofilament-like light chain 68 (*Nf68*; *Nefl* – Mouse Genome

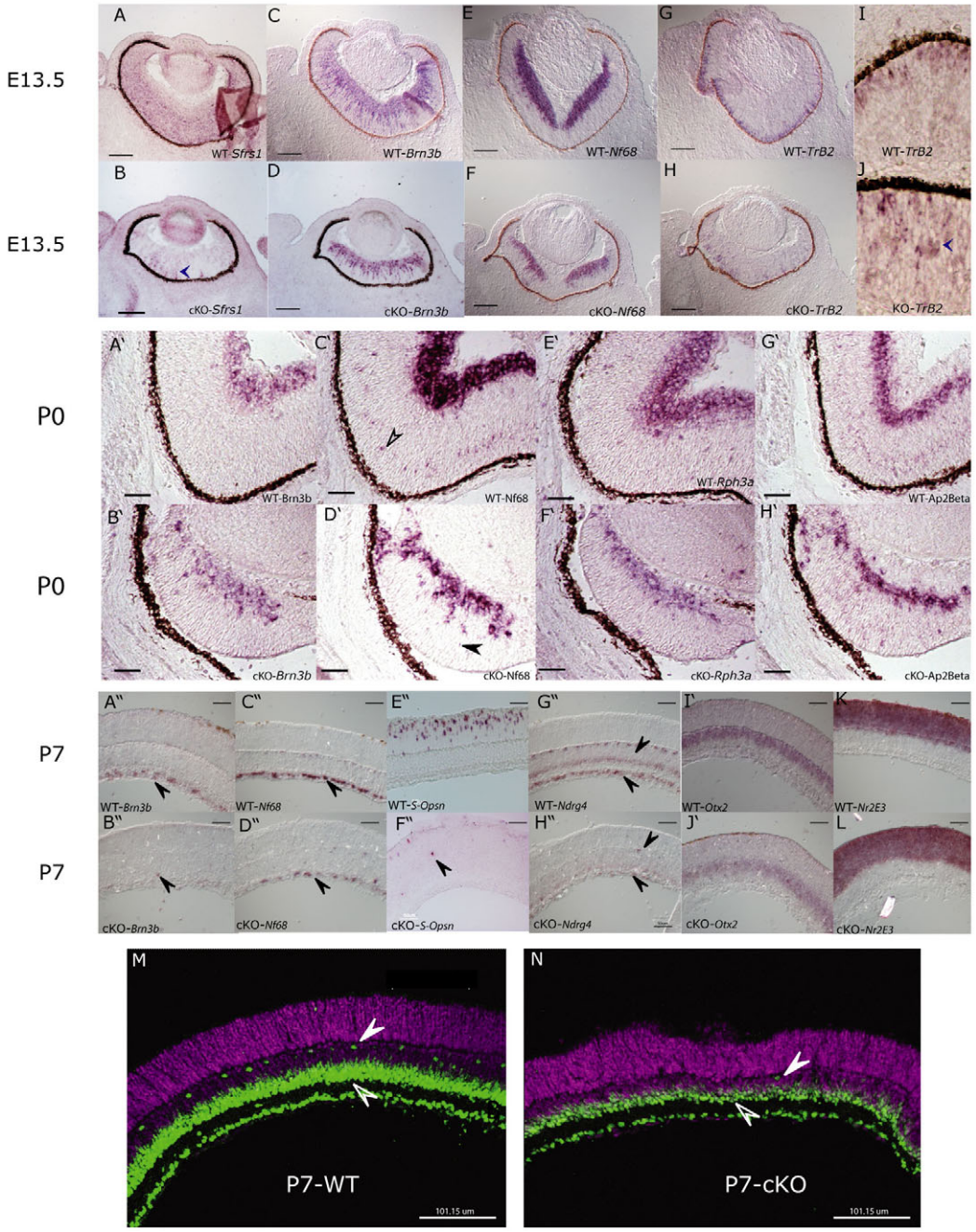

Fig. 5. Cell type composition in the *Sfrs1*-cKO retina. RNA ISH detecting *Sfrs1* (**A**,**B**), *Brn3b* (**C**,**D**), *Nf68* (**E**,**F**), *Trβ2* (**G**,**H**) RNA in E13.5 wild-type and *Sfrs1*-cKO mouse retinal sections. (**I**,**J**) Higher magnification images of the *Trβ2* ISH from G and H. RNA ISH detecting *Brn3b* (**A′**,**B′**), *Nf68* (**C′**,**D′**), *Rph3a* (**E′**,**F′**) and *Ap2b* (**G′**,**H′**) on P0 retinal sections. RNA ISH on P7 sections detecting *Brn3b* (**A″**,**B″**), *Nf68* (**C″**,**D″**), S opsin (**E″**,**F″**), *Ndrg4* (**G″**,**H″**), *Otx2* (**I′**,**J′**) and *Nr2e3* (**K**,**L**). Immunofluorescence for Pax6 (green) on P7 retinal sections stained with DAPI (magenta) (**M**,**N**). The white arrowhead indicates the horizontal cells, the open arrowhead points to the amacrine cells. Scale bars: 100 μm in A-H,A′-H′; 50 μm in A″-H″,I′,J′,K,L.

Informatics), brain 3b (*Brn3b*; *Pou4f2*) and thyroid hormone receptor beta 2 (*Trβ2*; *Thrb*). Ganglion cells were produced in the mutant retina, as shown by the strong ISH signal for *Nf68* and *Brn3b* (Fig. 5D,F). Similarly, cones were produced, as shown by the ISH signal for *Trβ2* in the *Sfrs1*-cKO retina (Fig. 5H). However, *Trβ2*$^{+}$ cone photoreceptors in the mutant retina were located throughout the ONBL (Fig. 5J, arrowhead), rather than abutting the RPE as was seen in the wild type (Fig. 5I). In summary, these data suggest that at least some neurons can be produced and initiate differentiation in the *Sfrs1*-cKO retina, with cones showing aberrant localization.

Neurons generated during early and mid-embryonic development die in the *Sfrs1*-cKO retina

To investigate the persistence of the neurons generated in the embryo, the above-mentioned strategy was employed on P0 retinal sections. This analysis showed that at P0, the ISH signal for *Brn3b*$^{+}$ and *Nf68*$^{+}$ ganglion cells was reduced in the *Sfrs1*-cKO retina (Fig. 5B′,D′). At P0, *Nf68* also labels horizontal cells (Fig. 5C′, arrowhead), which were significantly reduced in the *Sfrs1*-cKO retina (Fig. 5D′, arrowhead). Similarly, the ISH signal for rabphilin 3a (*Rph3a*) and

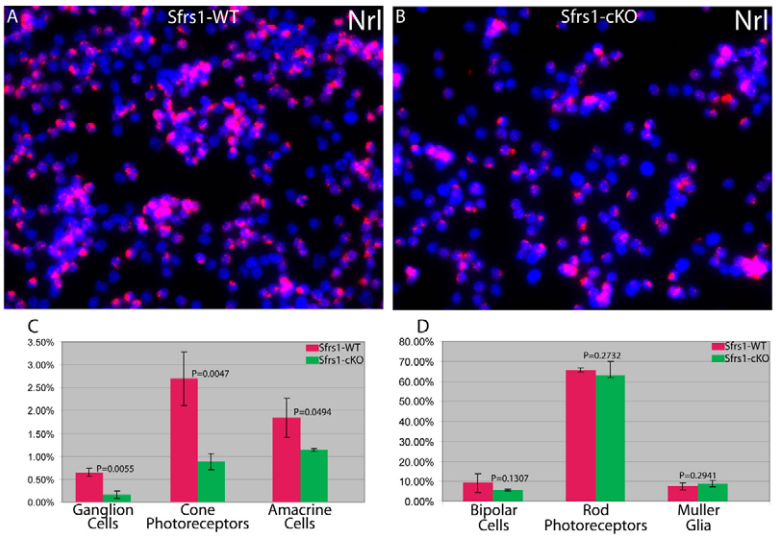

Fig. 6. Quantification of the different cell types in the *Sfrs1*-cKO retina. Quantification by dissociated in situ hybridization on P7 wild-type (n=3) and *Sfrs1*-cKO (n=3) mouse retinal cells with RNA probes for specific cell types. (**A**,**B**) Representative images of cells probed for *Nrl* (red) and stained with DAPI (blue). (**C**) The relative percentage of ganglion cells (*Nf68*), cone photoreceptors (short-wave opsin), and amacrine cells (*Pax6*) in wild-type and mutant retinae. (**D**) The relative percentage of bipolar cells (*Chx10*), rod photoreceptors (rhodopsin) and Müller glia (glutamine synthetase).

Ap2b, which mark amacrine cells, was also reduced (Fig. 5F′,H′). When we employed ISH with these and other probes at P7 to detect neurons produced in the embryo, very few of these neurons were detected. Specifically, there were few ganglion cells in the *Sfrs1*-cKO retina, as detected by ISH for *Brn3b* (Fig. 5B″, arrowhead) or *Nf68* (Fig. 5D″), the latter showing a few more ganglion cells than the former. In addition, cone cells [as determined by the S opsin (opsin 1) signal] were significantly reduced in number in the mutant retina (Fig. 5F″). Similarly, amacrine cells and horizontal cells were significantly reduced in the *Sfrs1*-cKO retina as determined by *Ndrg4* ISH (Fig. 5H″). Immunofluorescence with Pax6 revealed more amacrine cells than did the *Ndrg4* ISH, although numbers were still reduced compared with the wild type (Fig. 5M,N, open arrowhead). At P7, Pax6 antibody also marks horizontal cells, which were significantly decreased in the mutant retina (Fig. 5N, white arrowhead). By contrast, a similar reduction was not observed in cells produced postnatally. As shown by *Nr2e3* and *Otx2* ISH signal, the mutant retina did not exhibit a significant decrease in the thickness of the ONL, where the *Nr2e3*$^+$ rod photoreceptors primarily reside, or in the scleral half of the INL, where the postnatally generated *Otx2*$^+$ bipolar cells reside (Fig. 5J′,L). The significant decrease in the embryonically generated neurons was further quantified by dissociated cell in situ hybridizations (DISH) (Trimarchi et al., 2007). As shown in Fig. 6, by P7 there was a significant reduction in the number of embryonically generated neurons in the *Sfrs1*-cKO retina, which suggests that the cell death observed during embryonic development was most likely that of the postmitotic cells.

The conclusion that the loss of *Sfrs1* function led to the death of postmitotic cells was further investigated in a birthdating experiment. A pregnant female at E16 was injected with BrdU, followed by analysis at P7 of the *Sfrs1*-cKO retinae stained for BrdU and Pax6. The results showed a significant decrease in the number of heavily labeled BrdU$^+$ cells in the ONL, INL and GCL (Fig. 7). Here, the Pax6 antibody was used to mark amacrine cells, which are one of the major cell types produced at the time of the BrdU pulse. Quantification revealed that in the *Sfrs1*-cKO retina, there was a twofold decrease in the number of heavily labeled BrdU$^+$ cells as compared with its wild-type littermate (Fig. 7). This is in keeping with the death of postmitotic cells, although a failure to produce postmitotic cells in the normal numbers by *Sfr1*-cKO progenitor cells might also contribute to this deficit.

Sfrs1-cKO retinae undergo further degeneration during postnatal development

The neuronal composition of wild-type and *Sfrs1*-cKO retinae was compared at P14, a time when the production of retinal cell types is complete. Analysis at this stage revealed that the *Sfrs1*-cKO retina had undergone further degeneration and exhibited rosettes (Fig. 8D, arrowhead). Furthermore, in the mutant, the ciliary body was fused to the retina, such that it could not be separated from the neural retina (Fig. 8J, arrowhead), in contrast to the situation in the wild-type littermate where it was easily removed (Fig. 8I, arrowhead). Despite the severe morphological deterioration of the mutant retina at P14, it still appeared to have a relatively unaltered percentage of Müller glia as shown by IF with glutamine synthetase antibody (Fig. 8A,B). Similarly, rod photoreceptors also appeared relatively unaltered in the mutant retina (Fig. 8F, upper arrowhead; see Fig. S3 in the supplementary material). In contrast to the IF signals for Müller glia and rods, IF for Pax6 (Fig. 8F, lower arrowhead), Chx10 and red/green opsin showed a significant reduction in the *Sfrs1*-cKO retina (Fig. 8C,H). The reduction in the bipolar cells could be secondary to the loss of cone photoreceptors. This dysmorphic retina ultimately underwent complete degeneration by P30, as seen by the absence of the entire eye in the *Sfrs1*-cKO mouse (Fig. 8L). In summary, the data gathered at P14 indicate that despite the severe morphological defects observed in the mutant retina, cell types including rod photoreceptors, Müller glia and bipolar cells were relatively unaffected, whereas others, such as ganglion cells, amacrine cells, cone photoreceptors and horizontal cells, seemed to have undergone further loss.

Sfrs1 is not required for the maintenance of late-born neurons

P0 in vivo electroporation was used to investigate whether rod photoreceptors, Müller glia and bipolar cells were resistant to the loss of *Sfrs1* function. This strategy used two plasmids, one expressing Cre and the other expressing GFP in a conditional manner, such that it reported Cre activity. As shown in Fig. 8, production of rod photoreceptors was normal, and the rod photoreceptors had proper outer segments (Fig. 8M). In addition, amacrine cells appeared to be produced normally. Although bipolar cells and Müller glia were also produced during this time, the promoter driving GFP failed to express reproducibly in these two

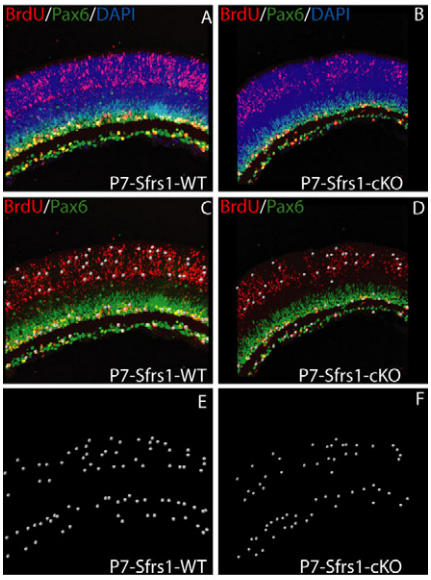

Retina	No. of BrdU Positive Cells
Sfrs1-WT #1	1425
Sfrs1-WT #2	1410
Sfrs1-WT #3	1401
Sfrs1-cKO #1	443
Sfrs1-cKO #2	480
Sfrs1-cKO #3	488

Fig. 7. Survival and/or production of neurons during embryonic development. (**A**,**B**) P7 retinal sections from wild-type and *Sfrs1*-cKO mice stained for BrdU (red), Pax6 (green) and with DAPI (blue). (**C**,**D**) Cells that were heavily labeled for BrdU were identified with an automated spot detection algorithm (IMARIS, Bitplane) utilizing a diameter threshold of 8 μm and pixel intensity threshold of 20.6 and are rendered as white spots. (**E**,**F**) The rendered spots shown without the fluorescence. The tabulated data beneath are the quantification of these spots.

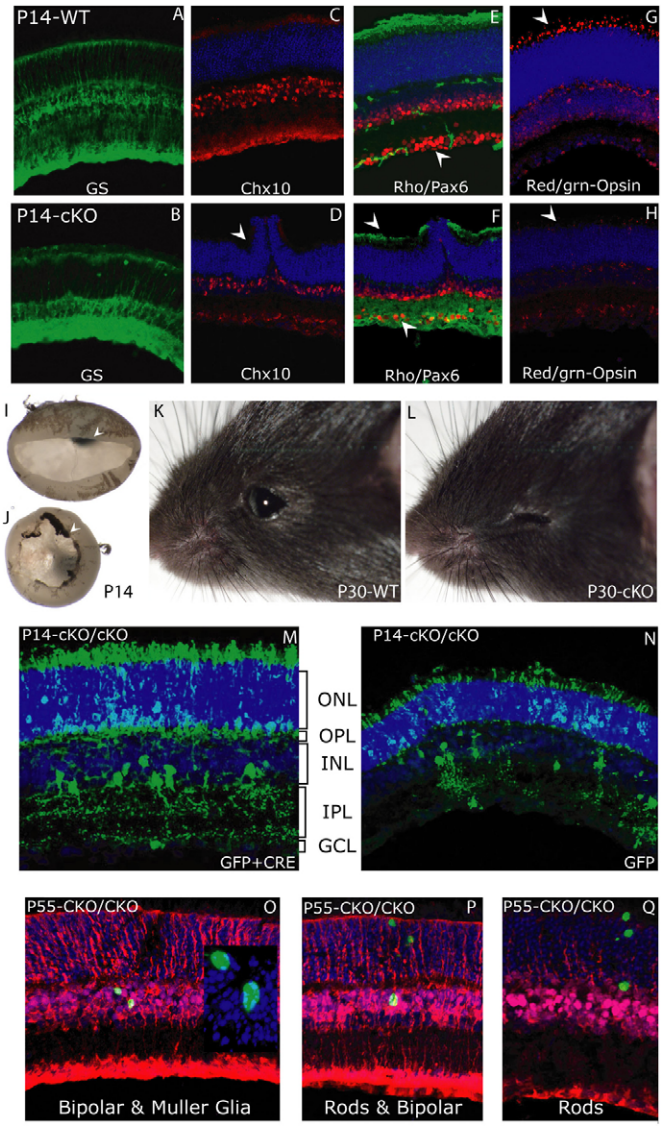

Fig. 8. Postnatal retinal development in the *Sfrs1*-cKO mouse. (**A-H**) Immunofluorescence on P14 wild-type and *Sfrs1*-cKO retinal sections with anti-glutamine synthetase (Müller glia) (A,B), anti-Chx10 (C,D), anti-rhodopsin (rod photoreceptors, top arrowhead) and anti-Pax6 (amacrine and horizontal cells, bottom arrowhead) (E,F), and anti-red/green opsin (cone photoreceptors) (G,H). (**I**,**J**) Wild-type and mutant retinae showing the ciliary margin attached to the mutant retina. (**K**,**L**) P30 wild-type and *Sfrs1*-cKO eyes. (**M**,**N**) Retinal sections stained with anti-GFP from P14 *Sfrs1*-cKO mice that were electroporated with Cre-GFP and LoxP-Stop-LoxP-GFP (M) or GFP alone (N) plasmids at P0. (**O-Q**) P55 retinal sections stained with anti-GFP (green) and anti-glutamine synthetase (red) antibody from mice that were infected with H2B-GFP-IRES-Cre virus at P0.

cell types, making it difficult to assess their relative levels. To investigate the production and maintenance of bipolar cells and Müller glia, the same virus used for embryonic ablation of *Sfrs1* was used to infect P0 retinal progenitor cells, followed by analysis at P55. Several nuclear GFP$^+$ clones were observed in the *Sfrs1*-cKO retina (Fig. 8O-Q). Based on the position and shape of the nuclei, the GFP$^+$ cells were judged to be rod photoreceptors, bipolar cells and Müller glia (Fig. 8O-Q; see Fig. S4 in the supplementary material). In summary, *Sfrs1* function is required in a temporal manner, such that neurons born postnatally are resistant to the loss of its function.

DISCUSSION

Sfrs1 is associated with the G2–M phase of the early retinal progenitor cell cycle and is itself temporally regulated via alternative splicing

During early embryonic development, *Sfrs1* RNA was enriched in the apical side of the retina (Fig. 1A), which suggests that it is associated with the M phase of the cell cycle. This was consistent with the overlapping expression patterns of *Cdc20* and PH3, both of which mark the M phase (see Fig. S1 in the supplementary material). Interestingly, a similar apical expression pattern for *Sfrs1* was observed in the olfactory epithelium (see Fig. S1 in the supplementary material). These data suggest that *Sfrs1* might regulate the G2–M phase transition in early progenitor cells. This is indeed the case in chicken DT-40 cells, in which loss of *Sfrs1* function results in G2 cell cycle block (Li et al., 2005).

Sfrs1, an ASF, is not only regulated at the transcriptional level during retinal development, but is also alternatively spliced in a temporal manner (Fig. 1). The newly identified isoform of *Sfrs1* includes intron 3, which produces a truncated isoform of Sfrs1 that would fail to translocate into the nucleus. This truncated isoform is

observed by immunoblot analysis and the GFP fusion version of this isoform is seen only in the cytoplasm. However, we cannot rule out the possibility that the new isoform is subject to nonsense-mediated mRNA decay and so the true identity of the lower molecular weight isoform warrants further investigation (see Fig. S5 in the supplementary material).

The importance of *Sfrs1* in retinal development is evidenced by the small and dysmorphic retinae in the *Sfrs1*-cKO mice (Fig. 2A). This phenotype is primarily a result of cell death during embryonic development (Fig. 3). Interestingly, this is in contrast to the role of *Sfrs1* in cardiac development, which proceeds normally during the embryonic period, whereas the postnatal remodeling of the heart is abnormal in *Sfrs1*-cKO mice, resulting in cardiomyopathy and death (Xu et al., 2005). It is interesting to note that the presence of the phenotype in the two tissues is correlated with the absence of the Sfrs1a isoform. In other words, the times at which the Sfrs1a isoform is expressed normally are the times when loss of Sfrs1 function does not result in a phenotype. One possibility is that another ASF that regulates the AS of *Sfrs1* normally compensates for the loss of *Sfrs1* function. Thus, the presence of Sfrs1a serves as a proxy for the presence of the compensatory ASF, which in the heart is present in the embryo, whereas in the retina it is present postnatally.

Sfrs1 loss-of-function results in the death of postmitotic cells

Progenitor cells in the *Sfrs1*-cKO retina did not die in significant numbers, as proliferation remained unaltered in the *Sfrs1*-cKO retina (Fig. 3A-H). In addition, infection of *Sfrs1*$^{fl/fl}$ progenitor cells with retrovirus expressing Cre and nuclear-GFP produced clones consisting mainly of later-born neurons (Fig. 4C). Similarly, several *nlacZ*$^{+}$ neurons were detected in the P7 mutant retina (Fig. 4E). The presence of *nlacZ*$^{+}$ cells reflects a history of Cre activity in the progenitor cells. These data indicate that the loss of *Sfrs1* function does not cause the death of the majority of retinal progenitor cells.

If the loss of *Sfrs1* function does not lead to the death of progenitor cells, then it must result in the death of postmitotic cells. This possibility is consistent with the pattern of TUNEL^{+} cells in the *Sfrs1*-cKO retinae. Specifically, the pattern of cell death overlaps with the production of postmitotic cells during development (Fig. 3) (Farah and Easter, 2005; Young, 1985a). Furthermore, ISH and IF analysis to detect differentiated neurons at P0 and P7 revealed that ganglion cells, horizontal cells, cone photoreceptors and amacrine cells were significantly reduced (Fig. 5). Interestingly, these neurons are produced in the embryo, coincident with the period of greatest cell death in the *Sfrs1*-cKO retina. By contrast, the later-born rod photoreceptors, bipolar cells and Müller glia were not as severely reduced (Figs 5 and 6). Taken together, these data indicate that in the *Sfrs1*-cKO retina, the postmitotic cells die in the embryo, which in turn could affect proliferation, as previous reports indicate that ganglion cell death can indirectly affect proliferation (Mu et al., 2005). However, in the case of the *Sfrs1*-cKO retina, which had reduced numbers of ganglion cells, there was little effect on proliferation (Fig. 5D). It is possible that the reduced numbers of ganglion cells were sufficient to produce the signals that might be crucial for proliferation.

The peak of amacrine cell production is ~E16.5-17.5, and production ends at ~P4 (Farah and Easter, 2005; Young, 1985a; Young, 1985b). Given that postnatally generated neurons are not affected in the *Sfrs1*-cKO retina, postnatally generated amacrine cells were not expected to die, which was reflected in the modest reduction in the Pax6 IF signal. By contrast, another marker of amacrine cells, *Ndrg4*, was significantly reduced in the mutant retina, which suggests that it marks the types of amacrine cells produced in the embryo. Based on this interpretation, we posit that there are at least two classes of amacrine cells as defined by their birthdate and subsequent dependence on *Sfrs1*, which warrants further investigation.

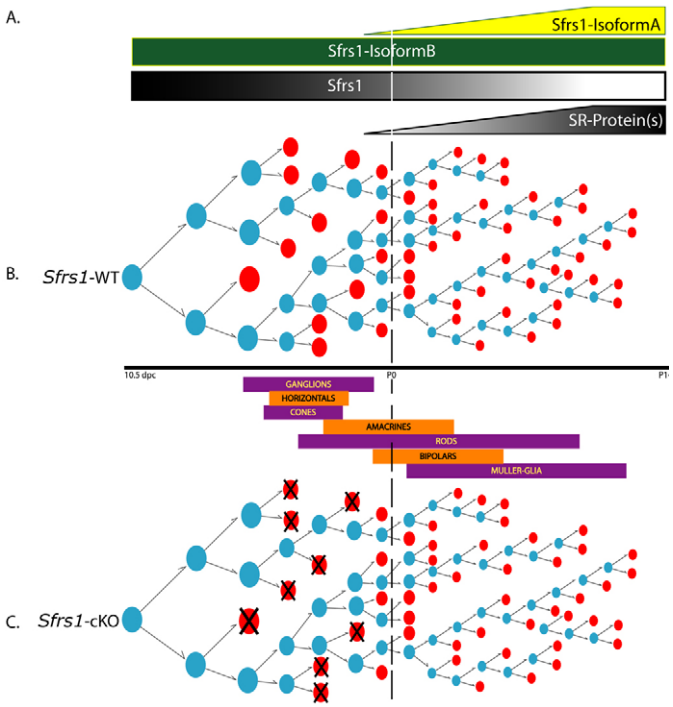

Fig. 9. Role of *Sfrs1* during mouse retinal development. (**A**) Expression pattern of the two Sfrs1 isoforms (Sfrs1a, Sfrs1b) during development and the requirement (dark gray) and the lack (light gray) of *Sfrs1* function. (**B**) A single progenitor in the wild-type retina is shown undergoing cell division and producing neurons and glia from E10.5 to P14. Mitotic cells are shown as blue ovals, and postmitotic cells as red ovals. The thick black line denotes time, with P0 (dashed line) indicating birth. Below the black line there are boxes depicting the birth order and the duration of each cell type. (**C**) A progenitor cell in the *Sfrs1*-cKO retina undergoing cell division and producing neurons, with crosses denoting cell death.

Unlike the aforementioned cell types, rod photoreceptors are born in significant numbers throughout retinal development. As discussed above, many of the early-born cells died prior to P0, which was also true for rod photoreceptors. As shown in Fig. 7, the number of BrdU^{+} cells in the ONL of the P7 *Sfrs1*-cKO retina was significantly reduced, suggesting that rod photoreceptors must have died. The remaining rod photoreceptors could be a consequence of *Chx10*::*Cre* mosaicism. It is unlikely that this reduction was due to the death of cone photoreceptors because very few (<5%) are produced at E16 (Carter-Dawson and LaVail, 1979). By contrast, rod photoreceptor production is initiated at ~E13 and by E16 more than 5% of the rod photoreceptors have been produced. Thus, like amacrine cells, rod photoreceptors produced in the embryo are most likely to die in the *Sfrs1*-cKO retina.

Temporal requirement of *Sfrs1* function for the survival of retinal neurons

In summary, the current investigation suggests that the key determinant of whether cells survive in the *Sfrs1*-cKO retina is when they are born, as opposed to the subtype of neuron. Several lines of

evidence point to this conclusion. First, the number of TUNEL$^+$ cells decreased late in embryonic development. Second, the genetic ablation of *Sfrs1* early in development led to the loss of many early-born neurons. This includes the early-born, but not the late-born, amacrine cells and rods. Third, survival of postnatal neurons was demonstrated by P0 electroporation of Cre and by P0 viral infection. Survival was coincident with the presence of the Sfrs1b isoform. Finally, we propose a model in which AS mediated by *Sfrs1* is required for the terminal differentiation and/or maintenance of neurons produced in the embryo, but not for neurons produced postnatally (Fig. 9). The data presented here underscore the dynamic role of ASFs during vertebrate neuronal development.

We thank Dr Xiang-Dong Fu for generously sharing the *Sfrs1* conditional knockout mouse. This project was funded by the Howard Hughes Medical Institute.

Supplementary material

Supplementary material for this article is available at
http://dev.biologists.org/cgi/content/full/135/23/3923/DC1

References

Caceres, J. F., Screaton, G. R. and Krainer, A. R. (1998). A specific subset of SR proteins shuttles continuously between the nucleus and the cytoplasm. *Genes Dev.* **12**, 55-66.

Carter-Dawson, L. D. and LaVail, M. M. (1979). Rods and cones in the mouse retina. II. Autoradiographic analysis of cell generation using tritiated thymidine. *J. Comp. Neurol.* **188**, 263-272.

Cepko, C. L. (1989). Immortalization of neural cells via retrovirus-mediated oncogene transduction. *Annu. Rev. Neurosci.* **12**, 47-65.

Cepko, C. L. (1996). The patterning and onset of opsin expression in vertebrate retinae. *Curr. Opin. Neurobiol.* **6**, 542-546.

Cheng, J., Kapranov, P., Drenkow, J., Dike, S., Brubaker, S., Patel, S., Long, J., Stern, D., Tammana, H., Helt, G. et al. (2005). Transcriptional maps of 10 human chromosomes at 5-nucleotide resolution. *Science* **308**, 1149-1154.

Davis-Silberman, N. and Ashery-Padan, R. (2008). Iris development in vertebrates: genetic and molecular considerations. *Brain Res.* **1192**, 17-28.

Farago, A. F., Awatramani, R. B. and Dymecki, S. M. (2006). Assembly of the brainstem cochlear nuclear complex is revealed by intersectional and subtractive genetic fate maps. *Neuron* **50**, 205-218.

Farah, M. H. and Easter, S. S., Jr (2005). Cell birth and death in the mouse retinal ganglion cell layer. *J. Comp. Neurol.* **489**, 120-134.

Gerdes, J., Li, L., Schlueter, C., Duchrow, M., Wohlenberg, C., Gerlach, C., Stahmer, I., Kloth, S., Brandt, E. and Flad, H. D. (1991). Immunobiochemical and molecular biologic characterization of the cell proliferation-associated nuclear antigen that is defined by monoclonal antibody Ki-67. *Am. J. Pathol.* **138**, 867-873.

Johnson, J. M., Castle, J., Garrett-Engele, P., Kan, Z., Loerch, P. M., Armour, C. D., Santos, R., Schadt, E. E., Stoughton, R. and Shoemaker, D. D. (2003). Genome-wide survey of human alternative pre-mRNA splicing with exon junction microarrays. *Science* **302**, 2141-2144.

Kampa, D., Cheng, J., Kapranov, P., Yamanaka, M., Brubaker, S., Cawley, S., Drenkow, J., Piccolboni, A., Bekiranov, S., Helt, G. et al. (2004). Novel RNAs identified from an in-depth analysis of the transcriptome of human chromosomes 21 and 22. *Genome Res.* **14**, 331-342.

Kanadia, R. N., Johnstone, K. A., Mankodi, A., Lungu, C., Thornton, C. A., Esson, D., Timmers, A. M., Hauswirth, W. W. and Swanson, M. S. (2003). A muscle blind knockout model for myotonic dystrophy. *Science* **302**, 1978-1980.

Kanadia, R. N., Shin, J., Yuan, Y., Beattie, S. G., Wheeler, T. M., Thornton, C. A. and Swanson, M. S. (2006). Reversal of RNA missplicing and myotonia after muscleblind overexpression in a mouse poly(CUG) model for myotonic dystrophy. *Proc. Natl. Acad. Sci. USA* **103**, 11748-11753.

Kataoka, N., Bachorik, J. L. and Dreyfuss, G. (1999). Transportin-SR, a nuclear import receptor for SR proteins. *J. Cell Biol.* **145**, 1145-1152.

Kawano, T., Fujita, M. and Sakamoto, H. (2000). Unique and redundant functions of SR proteins, a conserved family of splicing factors, in Caenorhabditis elegans development. *Mech. Dev.* **95**, 67-76.

Kawauchi, S., Shou, J., Santos, R., Hebert, J. M., McConnell, S. K., Mason, I. and Calof, A. L. (2005). Fgf8 expression defines a morphogenetic center required for olfactory neurogenesis and nasal cavity development in the mouse. *Development* **132**, 5211-5223.

Kim, D. S., Ross, S. E., Trimarchi, J. M., Aach, J., Greenberg, M. E. and Cepko, C. L. (2008). Identification of molecular markers of bipolar cells in the murine retina. *J. Comp. Neurol.* **507**, 1795-1810.

Lai, M. C., Lin, R. I., Huang, S. Y., Tsai, C. W. and Tarn, W. Y. (2000). A human importin-beta family protein, transportin-SR2, interacts with the phosphorylated RS domain of SR proteins. *J. Biol. Chem.* **275**, 7950-7957.

Lai, M. C., Lin, R. I. and Tarn, W. Y. (2001). Transportin-SR2 mediates nuclear import of phosphorylated SR proteins. *Proc. Natl. Acad. Sci. USA* **98**, 10154-10159.

Lareau, L. F., Inada, M., Green, R. E., Wengrod, J. C. and Brenner, S. E. (2007). Unproductive splicing of SR genes associated with highly conserved and ultraconserved DNA elements. *Nature* **446**, 926-929.

Li, X., Wang, J. and Manley, J. L. (2005). Loss of splicing factor ASF/SF2 induces G2 cell cycle arrest and apoptosis, but inhibits internucleosomal DNA fragmentation. *Genes Dev.* **19**, 2705-2714.

Livesey, F. J. and Cepko, C. L. (2001). Vertebrate neural cell-fate determination: lessons from the retina. *Nat. Rev. Neurosci.* **2**, 109-118.

Longman, D., McGarvey, T., McCracken, S., Johnstone, I. L., Blencowe, B. J. and Caceres, J. F. (2001). Multiple interactions between SRm160 and SR family proteins in enhancer-dependent splicing and development of C. elegans. *Curr. Biol.* **11**, 1923-1933.

Ma, C. T., Velazquez-Dones, A., Hagopian, J. C., Ghosh, G., Fu, X. D. and Adams, J. A. (2008). Ordered multi-site phosphorylation of the splicing factor ASF/SF2 by SRPK1. *J. Mol. Biol.* **376**, 55-68.

Matsuda, T. and Cepko, C. L. (2004). Electroporation and RNA interference in the rodent retina *in vivo* and *in vitro*. *Proc. Natl. Acad. Sci. USA* **101**, 16-22.

McCullough, R. M., Cantor, C. R. and Ding, C. (2005). High-throughput alternative splicing quantification by primer extension and matrix-assisted laser desorption/ionization time-of-flight mass spectrometry. *Nucleic Acids Res.* **33**, e99.

Molday, R. S. and MacKenzie, D. (1983). Monoclonal antibodies to rhodopsin: characterization, cross-reactivity, and application as structural probes. *Biochemistry* **22**, 653-660.

Mu, X., Fu, X., Sun, H., Liang, S., Maeda, H., Frishman, L. J. and Klein, W. H. (2005). Ganglion cells are required for normal progenitor- cell proliferation but not cell-fate determination or patterning in the developing mouse retina. *Curr. Biol.* **15**, 525-530.

Ni, J. Z., Grate, L., Donohue, J. P., Preston, C., Nobida, N., O'Brien, G., Shiue, L., Clark, T. A., Blume, J. E. and Ares, M., Jr (2007). Ultraconserved elements are associated with homeostatic control of splicing regulators by alternative splicing and nonsense-mediated decay. *Genes Dev.* **21**, 708-718.

Punzo, C. and Cepko, C. L. (2008). Ultrasound-guided in utero injections allow studies of the development and function of the eye. *Dev. Dyn.* **237**, 1034-1042.

Rapaport, D. H., Wong, L. L., Wood, E. D., Yasumura, D. and LaVail, M. M. (2004). Timing and topography of cell genesis in the rat retina. *J. Comp. Neurol.* **474**, 304-324.

Rivera-Feliciano, J. and Tabin, C. J. (2006). Bmp2 instructs cardiac progenitors to form the heart-valve-inducing field. *Dev. Biol.* **295**, 580-588.

Rowan, S. and Cepko, C. L. (2004). Genetic analysis of the homeodomain transcription factor Chx10 in the retina using a novel multifunctional BAC transgenic mouse reporter. *Dev. Biol.* **271**, 388-402.

Seki, M., Narusaka, M., Kamiya, A., Ishida, J., Satou, M., Sakurai, T., Nakajima, M., Enju, A., Akiyama, K., Oono, Y. et al. (2002). Functional annotation of a full-length Arabidopsis cDNA collection. *Science* **296**, 141-145.

Sidman, R. L. (1961). Histogenesis of mouse retina studied with Thymidine-H-3. In *The Structure of the Eye* (ed. G. K. Smelser), pp. 487-506. New York, NY: Academic Press.

Trimarchi, J. M., Stadler, M. B., Roska, B., Billings, N., Sun, B., Bartch, B. and Cepko, C. L. (2007). Molecular heterogeneity of developing retinal ganglion and amacrine cells revealed through single cell gene expression profiling. *J. Comp. Neurol.* **502**, 1047-1065.

Trimarchi, J. M., Stadler, M. B. and Cepko, C. L. (2008). Individual retinal progenitor cells display extensive heterogeneity of gene expression. *PLoS ONE* **3**, e1588.

Weinstein, J. (1997). Cell cycle-regulated expression, phosphorylation, and degradation of p55Cdc. A mammalian homolog of CDC20/Fizzy/slp1. *J. Biol. Chem.* **272**, 28501-28511.

Xu, X., Yang, D., Ding, J. H., Wang, W., Chu, P. H., Dalton, N. D., Wang, H. Y., Bermingham, J. R., Jr, Ye, Z., Liu, F. et al. (2005). ASF/SF2-regulated CaMKIIdelta alternative splicing temporally reprograms excitation-contraction coupling in cardiac muscle. *Cell* **120**, 59-72.

Young, R. W. (1985a). Cell differentiation in the retina of the mouse. *Anat. Rec.* **212**, 199-205.

Young, R. W. (1985b). Cell proliferation during postnatal development of the retina in the mouse. *Brain Res.* **353**, 229-239.

Zahler, A. M. (1999). Purification of SR protein splicing factors. *Methods Mol. Biol.* **118**, 419-432.

Zahler, A. M., Lane, W. S., Stolk, J. A. and Roth, M. B. (1992). SR proteins: a conserved family of pre-mRNA splicing factors. *Genes Dev.* **6**, 837-847.